INFORMATICA, 2011, Vol. 22, No. 2, 259–278

A Serial-Parallel Panoramic Filter Bank as a Model of Frequency Decomposition of Complex Sounds in the Human Inner Ear

Antanas STASIŪNAS[1], Antanas VERIKAS[1,2] *,
Rimvydas MILIAUSKAS[3], Marija BAČAUSKIENĖ[1]

[1]*Department of Electrical and Control Equipment, Kaunas University of Technology*
Studentų 50, LT-51368 Kaunas, Lithuania
[2]*Intelligent Systems Laboratory, Halmstad University*
Box 823, S-30118 Halmstad, Sweden
[3]*Department of Physiology, Lithuanian University of Health Sciences*
A. Mickevičiaus 9, LT-44307 Kaunas, Lithuania
e-mail: antanas.stasiunas@ktu.lt, antanas.verikas@hh.se, milius@med.kmu.lt, marija.bacauskiene@ktu.lt

Received: January 2010; accepted: October 2010

Abstract. We consider that the outer hair cells of the inner ear together with the local structures of the basilar membrane, reticular lamina and tectorial membrane form the primary filters (PF) of the second order. Taking into account a delay in transmission of the excitation signal in the cochlea and the influence of the Reissner membrane, we design a signal filtering system consisting of the PF with the common PF of the neighboring channels. We assess the distribution of the central frequencies of the channels along the cochlea, optimal number of the PF constituting a channel, natural frequencies of the channels, damping factors and summation weights of the outputs of the PF. As an example, we present a filter bank comprising 20 Gaussian-type channels each consisting of five PF. The proposed filtering system can be useful for designing cochlear implants based on biological principles of signal processing in the cochlea.

Keywords: inner ear, outer hair cell motility, lateral inhibition, panoramic filter-bank, cochlear implants.

1. Introduction

Preliminary processing of the sound signals is performed in the cochlea of the inner ear of the peripheral auditory system. The processing consists of the multi-channel band-pass filtering of the complex signals, transduction of the filtered signals into nerve impulses and their transmission to the higher auditory centers. On the basis of the anatomical, physiological and biochemical data accumulated over decades it seems reasonable to assume that the multi-channel band-pass filtering system of the cochlea consists of the

*Corresponding author

local passive structures of the tectorial membrane (TM), reticular lamina (RL), basilar membrane (BM) and the active outer hair cells (OHC) of the Corti organ interposed between RL and BM. The passive structures are not distinctive with their sensitivity and selectivity as shown by vibrations of the BM in cadaver cochlea (von Bekesy, 1960). The amplitudes of vibrations of the BM, however, are hundredfold higher with the living OHC (Rhode, 1971). Thus, the OHC interacting with the passive structures of the cochlea and between one another and having afferent as well as efferent connections with the higher auditory centers improve characteristics of the filtering system. The systematic mapping of frequencies upon longitudinal position on the BM (von Bekesy, 1960; Greenwood, 1990) and systematic variations of dimensions of the OHC, stiffness and size of the BM and TM (Spector *et al.*, 1999; Robles *et al.*, 2001; Sugawara *et al.*, 2001) suggest that the OHC together with the local passive structures can be regarded as a primary panoramic filter bank.

Many different models were proposed during different periods of studies to explain high sensitivity and selectivity of the auditory system. The attention was concentrated on the active role of the OHC in the cochlea of the inner ear (Gold, 1948; Kemp, 1978; Davis, 1983; Janušauskas *et al.*, 2010), suggesting that they could work as the "cochlear amplifier" (Ashmore, 1987, 2008; Dallos *et al.*, 1995, 2006). The discovery of the motility of the OHC (Brownell *et al.*, 1985) contributed fundamentally to understanding of the active processes in the cochlea. Until that time experimental data were lacking to explain the role of the OHC in the cochlear models with linear and non-linear feedback (Allen, 1979; Zwicker, 1979; Neely *et al.*, 1983).

Even after discovery of the motility of OHC additional 15 years were necessary to reveal the responsible motor protein prestin (Zheng *et al.*, 2000). The discovery of prestin contributed essentially to a better understanding of the cochlear amplifier and the role of the OHC. Nevertheless, the mechanism controlling conformational changes of prestin and changes in length of the OHC remain uncertain since the high frequency components of the receptor potential might be shunted by the RC filter of the OHC membrane (Russell *et al.*, 1983; Preyer *et al.*, 1996). Consequently, fast oscillations in membrane potential could not be responsible for changes in length of the OHC at high frequencies of 80–100 kHz (Ashmore, 1987; Santos-Sacchi, 1992; Frank *et al.*, 1999; Scherer *et al.*, 2004).

An alternative possibility is that the mammalian filtering system is based on the active hair bundle motion of the OHC similar to that found in the reptiles (Crawford *et al.*, 1985; Hudspeth *et al.*, 1997; Manley, 2001; Ricci, 2003; Chan *et al.*, 2005a; Kennedy *et al.*, 2005). The new experimental data, however, required corrections of this view (Jia *et al.*, 2005; Chan *et al.*, 2005b; Kennedy *et al.*, 2006).

The fast conformational changes of prestin and changes in length of the OHC could be controlled by the extracellular potential (Dallos *et al.*, 1995; Fridberger *et al.*, 2004). There is also another possibility that shunting of the membrane potential could be compensated by a negative feedback (Lu *et al.*, 2006). The question is still not finally resolved.

Although the somatic motility of the OHC can be the basis of the cochlear amplifier (Dallos *et al.*, 2008a; Stasiunas *et al.*, 2009), the control mechanism of the motor protein prestin still needs to be substantiated (Dallos, 2008b). In addition to individual activity

of a single OHC the electrical-mechanical interaction between the OHC manifested that the lateral inhibition is important for the filtering system of the cochlea (Nobili *et al.*, 1998; Zhao *et al.*, 1999; Stasiunas *et al.*, 2008). It means that excitation of an individual OHC is accompanied by inhibition of neighboring OHC. Unfortunately, this issue was not sufficiently studied. Little is known about the relations between the control of OHC length and the lateral inhibition although the existence of their interaction is really plausible. Therefore significant advances are expected to be made in the next 50 years or so (Evans *et al.*, 2006).

A significant contribution to better understanding of functional principles of the peripheral auditory system is provided by the functional computer modeling. This method helps to explain, at least qualitatively, experimental findings and to predict the new functional peculiarities of the biological structures of the cochlea. For example, in a model of OHC with non-linear feedback we approximated the characteristic of the mechanical-electrical transduction (MET) to the hyperbolic tangent function (Stasiunas *et al.*, 2003). This function, in contrast to the widely used Boltzman function, enabled us to relate the shift of the parameter along the abscissa with the inclination of the hair bundle, to realize the biological meaning of the initial position of the bundle and to estimate the influence on the characteristics of the primary filter (PF). In another model (Stasiunas *et al.*, 2005) we showed how the characteristics of the PF are changed by the parameters of the mechanomotility (Evans *et al.*, 1993) of the OHC: the shift of the transfer characteristic of the MET and the coefficient of the transfer characteristic of the electromechanical transduction (EMT). We provided the biological interpretation of these parameters as the inclination of hair bundle and the stiffness of the lateral wall of the OHC. In still another model (Stasiunas *et al.*, 2009) we showed how the motility of the OHC included in the PF improves the sensitivity and selectivity of the filter. Obviously, the direct component (DC) of the receptor potential, the inclination of the hair bundle and the stiffness of the lateral wall of the OHC thus adjusting the characteristics of the PF to the changed intensity of the input signal or to the efferent synaptic action. On the basis of biological data and our own assumptions we assessed the relations between two types of mechanical motility of the OHC and their functions in the PF of the cochlear filtering system by means of computer modeling. We showed that the main mechanism for the realization of filtering is the motility of the OHC. At higher signal intensities, however, the mechanism of OHC bundle motion comes into play decreasing the sensitivity and selectivity of the filtering system. Nevertheless, the relation between the two amplification processes still remains one of the main problems in mammalian cochlear physiology (Dallos, 2008).

In the present work we designed a qualitative functional model of the filtering system in the cochlea based on the distribution of the OHC and IHC, the lateral interaction of the OHC, experimental data of many authors, and our own assumptions. We used non-linear PF of the second order as elements of the system consisting of interacting OHC and passive local structures of the cochlea (Stasiunas *et al.*, 2009). Using approximation proposed by Greenwood (1990, 1996) and the hexagonal arrangement of OHC on the BM we defined locations of the OHC. We determined a rational number of PF in a Gaussian filtering channel, their natural frequencies and damping factors. To illustrate the properties of the model we designed a panoramic filter bank (PFB) made up of 20 channels each

consisting of five PF. The results allowed us to conclude that our model can be useful in designing PFB for auditory implants based on biological principles (Gao *et al.*, 2003; Wilson *et al.*, 2005; Clark, 2006).

2. Material and Methods

2.1. *Distribution of the OHC in the Cochlea*

The auditory sensory receptors are the inner hair cells (IHC) and outer hair cells (OHC) in the cochlea. OHC are included in the primary filters (PF) as feedback elements increasing the sensitivity and selectivity of filters. Oscillations evoked by the PF in the endolymph excite the IHC located in front of the OHC. The IHC release a neurotransmitter exciting the afferent nerve fibers carrying the nerve impulses to the spiral ganglion and to the cochlear nuclei in the brainstem. IHC are distributed in one row on the BM while the OHC are distributed in three rows (in some places can be even four or five rows). The number of OHC (about 12,000) is more than three times the number of IHC (about 3,500) (Gray's Anatomy, 2005). Scanning electron microscopic images show almost hexagonal arrangement of the OHC (e.g., Figs. 13–20 in Boron *et al.* (2003)). A particular IHC is approximately lined up against the OHC of the middle row. The length of the human BM is about 35 mm. The width of the BM increases from 0.21 mm at the base of the cochlea near the stapes to 0.36 mm at the apex of the cochlea (Gray's Anatomy, 2005). The length of the OHC and their steriocilia increases and the stiffness decreases from the stapes to the apex of the cochlea (Spector *et al.*, 1999; Sugawara *et al.*, 2001; Robles *et al.*, 2001). We used hexagonal principle (Fig. 1a), the known parameters of the human BM (length L_m, width at the stapes d_s and at the apex d_a), and the number of IHC N_m for modeling the distribution of the OHC on the BM with equal distances between them in a row and with distances increasing linearly and non-linearly. Such distributions with a linear increase of distances are shown at stapes, at the midway of the BM and at the apex (Fig. 1b).

Although differences between these parts are appreciable, it is difficult to notice them in short segments of scanning electron microscopic images of Corti organ. Nevertheless, these images show that the distances between cell rows are significantly larger than the distances between neighboring cells of the same row. This means that the hexagonal structure is stretched in the radial direction. In addition, the corresponding OHC of the first and the third row are shifted a little relatively to one another.

When modeling hexagonal arrangement of the OHC, we used the recurrent algorithm to find the distances between neighboring cells along the BM. First of all, according to the location L_k (distance from the stapes) of a given OHC of the middle row, we define the distance between the outer rows:

$$d_k = K_m\big(d_s + \alpha(L_k)L_k\big), \tag{1}$$

where $\alpha(L_k)$ defines the mode of widening of the BM and K_m is the coefficient of distortion of the hexagonal structure along or across the BM. Next, according to (1) and

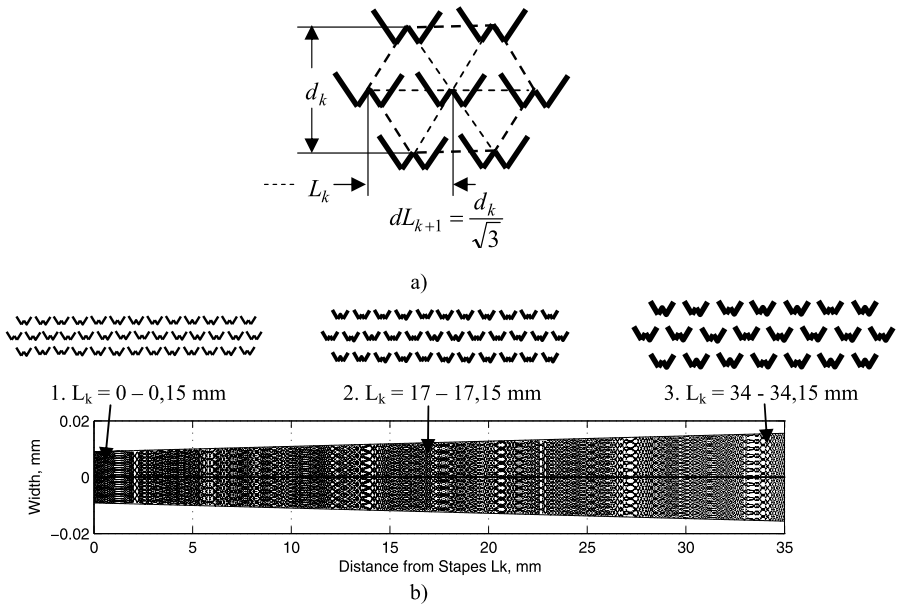

Fig. 1. The relations of measurements of the hexagonal arrangements of the OHC. (a) A model of distribution of the OHC on the BM with a linear increase of distances between the OHC in a row: at stapes (1), at the midway (2) and at the apex (3) of the cochlea. (b) Distribution of the OHC along the whole length of the BM. Here the OHC are distributed at max/min and zero crossing points of two sinus functions with opposite polarity: $y_{1k} = d_k(L_k)\sin[2\pi F_0 L_k - 3\pi\alpha_l L_k^3]$, where the envelope $d_k(L_k) = K_m[d_s/2 + \alpha_l L_k]$ determines the mode of widening of the BM, F_0 determines the initial distance between neighboring OHC and $\alpha_l = (d_a - d_s)/2L_m$ is the coefficient of widening of the BM and of increase in the distance between cells. The presented distribution corresponds to $d_s = 0.21$ mm, $d_a = 0.36$ mm, $L_m = 35$ mm. The values $F_0 = 50$; $K_m = 0.0866$; $\alpha_l = 0.00214$ were obtained by computer modeling to match changes in amplitudes and frequencies of the sinus functions for hexagonal distribution of the OHC in three rows with 3,100 cells in each.

the attributes of the hexagonal arrangement (Fig. 1a), we find the distance between the OHC located at L_k and the next cell in the middle row:

$$dL_{k+1} = d_k/\sqrt{3}. \tag{2}$$

Then we find the location (distance from the stapes) of that cell:

$$L_{k+1} = L_k + dL_{k+1}. \tag{3}$$

In the next step, assuming the new $L_k = L_{k+1}$ and using (1)–(3), we can find L_{k+2} and so on. This recurrent algorithm and computer modeling were used to define the dependence of the number of cells N_k (Fig. 2a) and the distance between the neighboring cells dL_k (Fig. 2b) on the distance from the stapes L_k. The graphs show the dependences of N_k and dL_k when the distances between cells are constant (lines 0), when they change linearly (curves 1) and non-linearly (curves 2).

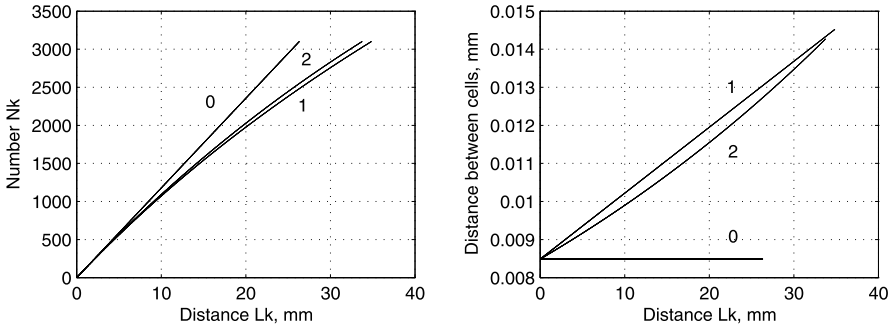

a) b)

Fig. 2. Dependences of the number of cells N_k (a) and the distance between the neighboring cells dL_k (b) on the distance from the stapes. When widening of the BM is linear, its width is $d_k = K_m(d_s + \alpha_l L_k)$, where $\alpha_l = (d_a - d_s)/L_m$ is the coefficient of the linear widening, and the distances between cells dL_{k+1} in a row also change linearly. The way they change is well approximated by a linear equation $dL_{k+1} = a + bL_k$ with the coefficients $a = 0,00848$ and $b = 0,000173$ (line 1). When widening of the BM is exponential, its width is $d_k = K_m d_s \exp(\alpha_s L_k)$, where $\alpha_s = \ln(d_a/d_s)/L_m$ is the exponential coefficient of widening, and the distances between the cells in a row dL_{k+1} increase non-linearly. The way they change is well approximated by a non-linear equation $dL_{k+1} = a + bL_k + cL_k^2$ with the coefficients $a = 0,00848,\ b = 0,0001265$ and $c = 0.000001315$ (curve 2). The following values were used for the graphs: $d_s = 0,21$ mm, $d_a = 0,36$ mm, $d_a = 0,36$ mm, $L_m = 35$ mm, $K_m = 217/N_m$, and $N_m = 3100$.

A comparison of exponential (curve 2) and linear (curve 1) widening of the BM shows (Fig. 2a) that the BM contains more OHC in case of linear widening. It could contain even more if the OHC were distributed at equal distances from one another (line 0). However, such distribution is unlikely to happen. Therefore we assume that exponential widening of the BM and the corresponding non-linear distribution of the OHC are closer to the biological case.

2.2. *Distribution of the Characteristic Frequency (CF)*

Each OHC has its own place on the BM and each site of the BM has a characteristic frequency (CF), to which it is most sensitive. The intervals between the OHC and the intervals between the CF change according to a certain law. We estimated that the distances between the OHC increase non-linearly if widening of the BM is exponential. It is not known, however, how the distances between the neighboring frequencies change with changing distances between the OHC.

The dependence of the CF on the distance along the mammalian BM can be expressed by an equation proposed by Greenwood (1990):

$$(\mathrm{CF})_{\mathrm{apex}} = A\big[10^{\alpha x} - K\big]. \tag{4}$$

Here the distance x is measured from the apex and the constants suitable for human cochlea are the following: $A = 165,\ \alpha = 0.06$ and $K = 1$. It was established that the

frequencies $(\mathrm{CF})_{\mathrm{apex}}$ are distributed according to a near-logarithmic law (von Bekesy, 1960; Robles *et al.*, 2001).

By substituting $x = L_m - L_k$, where L_m is the length of the BM and L_k is the cell distance from the stapes found by the recurrent algorithm (1)–(3), we obtain the equation for finding the CF:

$$F_k = A\big[10^{\alpha(L_m - L_k)} - K\big]. \tag{5}$$

The values of the constants $A,\ \alpha$ and K are the same as in (4) and $L_m = 35$ mm (Gray's Anatomy, 2005).

The equation (4) gives a continuous dependence of CF on the distance along the BM. Since the distribution of the OHC on the BM is discrete, the distribution of corresponding frequencies F_k is also discrete. Thus, after assessment of the location L_k of the OHC using the recurrent algorithm (1)–(3), it is possible to determine the corresponding discrete values of the frequencies F_k using (5). Consequently it is possible to define the intervals between neighboring frequencies depending on their location along the BM using (5).

2.3. *Characteristics of the Primary Filters (PF) and Distribution of Their Parameters Along the Cochlea*

The active OHC together with the surrounding passive structures of the cochlea (BM, RL and TM) make up non-linear primary filters (PF) of the second order. The location of the PF is determined by the location of the OHC. Non-linearities of the PF are insignificant at low signal level and therefore the PF can be characterized by transfer functions of the second order (Stasiunas *et al.*, 2009). The parameters of these functions are the natural frequency and damping. We assume that characteristic frequencies F_k of the BM correspond to the natural frequencies f_k of the PF, and the geometric mean of the neighboring characteristic frequencies $dF_k = \sqrt{(F_k - F_{k+1})(F_{k+1} - F_{k+2})}$ corresponds to the bandwidth df_k of the PF. Then the quality Q_k and damping ξ_k of the PF can be found using the equations:

$$Q_k = f_{k+1}/df_k, \tag{6}$$

$$\xi_k = 1/2Q_k. \tag{7}$$

The frequency response of the PF in ranges 200–2,000 Hz and 2,000–10,500 Hz are shown in the upper part of Fig. 3. For computer modeling we considered the PF as the filters of the second order and assumed their number to be 56 in the range of 16–20,000 Hz. The dependences of the discrete natural frequencies f_k and qualities Q_k on the distance from the stapes are shown in the bottom part of Fig. 3. They were found using the recurrent algorithm (1)–(3) and (5) and (6). As can be seen, the frequency characteristics intersect at the level of 0.7, the distribution of the natural frequencies f_k is near-logarithmic and the qualities Q_k decrease toward the apex of the cochlea.

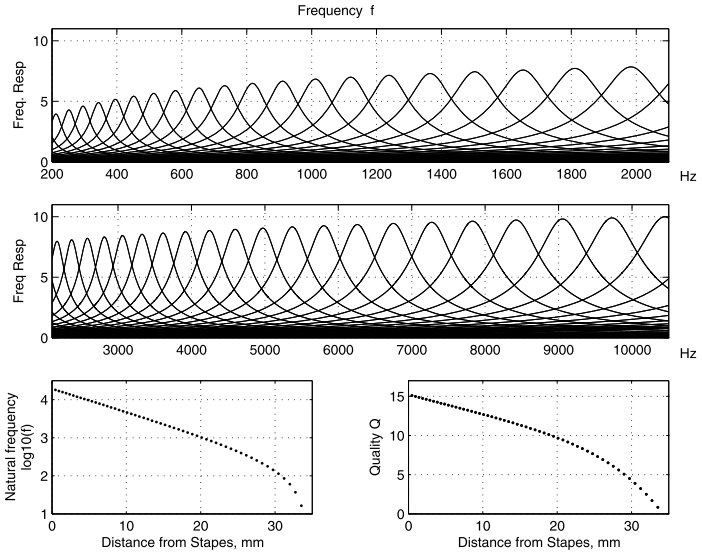

Fig. 3. Frequency responses of primary filters in the range of 200–10,500 Hz, and dependences of natural frequency logarithm $\log_{10}(F_k)$ and quality Q_k on the distance from the stapes.

3. The Model of the Filtering System of the Cochlea

3.1. *The Qualitative Functional Model*

Based on the anatomical-physiological peculiarities of the cochlea and distribution of the hair cells in Corti organ, a serial-parallel structure of the peripheral filtering system was designed (Fig. 4). The line consisting of discrete delay elements D_k models propagation and delay of sound-evoked excitation signal in the cochlea. The side-branches of the delay line represent signal transmission changes across the thin Reissner membrane in the transverse (vertical) direction. Their output signals x_k act on the passive local structures TM, RL and BM between which the OHC are interposed. We model these structures by non-linear primary band-pass filters of the second order (Stasiunas *et al.*, 2009).

In the functional model (Fig. 4), an OHC from the middle row is included in, let's say, odd PF. The natural frequencies of these filters correspond to the central frequencies of the channels. Meanwhile, OHC from the first and third rows located approximately at the same distance from the stapes are included in the even channels. They can be considered as having the same natural frequency. Therefore a filtering channel in the scheme consists of five PF instead of six. The PF of neighboring channels are common. Their contribution to the channel is evaluated by weight coefficients C_{k-i} $(i = 0, \pm1, \pm2, \pm3, \ldots)$ depending on the number of PF. The module of the coefficient shows the contribution of the PF to the output signal $z_k(t)$ of the channel, and the sign shows an exciting or damping effect. The signs of summation coefficients of the output signals of all even PF are negative (Fig. 4) and those of odd PF are positive (or vice versa). In such a way we estimate the lateral inhibition between the neighboring OHC as well as the PF formed by them.

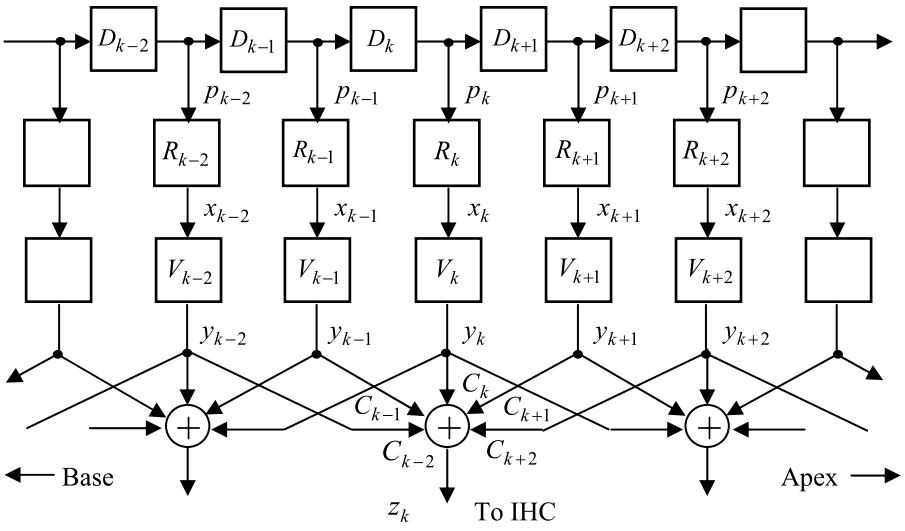

Fig. 4. Functional model of signal transmission in a biological filtering system consisting of delay circuits D_{k-i}, passive filters R_{k-i}, and active primary filters V_{k-i} ($k = 5, \ldots;\ i = 0, \pm 1, \pm 2$).

However, if the OHC in the first and third rows are shifted relatively to one another, then the channel would consist of six PF. For the sake of simplicity, we assume that such a shift is absent.

The primary filters W_k of the filtering system of the cochlea are non-linear. They model biological filters which include OHC linked to the higher auditory centers by afferent and efferent connections. There are no doubts now that the somatic motility of the OHC plays the main role in realizing selective filtering while another mechanism, the hair bundle motion, is important for adaptation process during transition to the non-linear mode at higher sound levels (Stasiunas *et al.*, 2009).

The signal transmission from the stapes in the linear mode can be defined by the product of the multipliers representing the signal delay and the transfer functions of the first and second order:

$$W_k(s) = T_k(s)R_k(s)V_k(s). \tag{8}$$

The first term in (8) estimates the delay of the excitation signal up to the kth filtering circuit:

$$T_k(s) = \exp(-\tau_k s). \tag{9}$$

The second term in (8) estimates the signal transfer across Reissner membrane to the endolymph:

$$R_k(s) = \frac{\omega_{rk}}{s + \omega_{rk}}. \tag{10}$$

The third term in (8) represents the transfer function of the active PF including the OHC:

$$V_k(s) = \frac{\omega_{vk} s}{s^2 + 2\omega_{vk}\xi_{wk} s + [\omega_{vk}]^2}. \tag{11}$$

In the above expressions, $s = \sigma + j\omega$ ($j = \sqrt{-1}$) is a complex variable, ω_{rk} and ω_{vk} are the natural frequencies of Reissner membrane and the passive local structures (BM-RL-TM) of the cochlea, respectively, and ξ_{wi} is the equivalent damping factor of the active PF including the OHC.

The physical dimensions and parameters of the constituents of the filtering system change continuously from the base to the apex of the cochlea. The excitation signal delay and the inertia of Reissner membrane influence the transmission of the spectral components of a complex signal to the endolymph of the cochlea. These parameters are associated with the natural frequencies of the PF.

Let's assume that the delay of the excitation signal $p_k(t)$ is inversely proportional to the natural corner frequency:

$$\tau_k = 1/\omega_k. \tag{12}$$

Reissner membrane (RM) is quite thin therefore is considered as having no significant effect on the serial-parallel transmission of the signal from the perilymph in scala vestibuli to the endolymph in the cochlear duct. However the physical dimensions of the RM change in a wide range from the stapes to the apex (Gray's Anatomy, 2005). It is a logical suggestion that the parameters of these changes are related linearly to the parameters of the discrete PF.

Let's assume that

$$\omega_{rk} = \omega_{vk}. \tag{13}$$

The kth filtering channel is formed of several PF. The number of the PF depends on the type of the channel. In general, the transfer function of a symmetrical channel consisting of M primary filters ($M = 3, 5, 7, \ldots$) is the following:

$$G_k(s) = \sum_{i=-(M-1)/2}^{(M-1)/2} C_{k-i} W_{k-i}(s). \tag{14}$$

The weight coefficients for a channel symmetrical relative to the central frequency are selected in such a way that the sum of the weights C_{k-i} of the output signals would be equal to zero. For example, when designing a channel consisting of five PF the following relations between the summation coefficients can be used: $C_{k-2} = C_{k+2} = c$; $C_{k-1} = C_{k+1} = -4c$; $C_k = 6c$, where the constant multiplier c is a real positive or negative number. The biological meaning of c is not clear.

3.2. *The Number of the Primary Filters and the Damping Factors of a Gaussian Channel*

The number of the PF in a channel, their natural frequencies and damping depend on the frequency and time characteristics of the channel in a serial-parallel filtering structure (Fig. 4). It is well-known that Gaussian filters are distinctive in their frequency selectivity and short transient process. Therefore it is reasonable to assume that the biological filtering channels of the cochlea are Gaussian, and the exponential widening of the BM and hexagonal arrangement of the OHC are close to reality.

We designed the channels consisting of M primary filters ($M = 1, 3, 5, 7, 9$) using the model of the filtering system (Fig. 4). The summation weight of their output signals, their natural frequencies and primary damping are given in Table 1. The natural frequencies and primary damping were determined for 128 PF in the range of 16–20,000 Hz using the recurrent algorithm (1)–(3) and (7). In order to design Gaussian channels, it is necessary to increase primary damping of the PF (Table 1, Damp) by multiplier h.

We compared these characteristics with the graphical charts of Gaussian frequency and time functions:

$$G(x) = \frac{A_x}{dx\sqrt{2\pi}} \exp\left(- \frac{(x - x_0)^2}{2(dx)^2} \right). \tag{15}$$

Here x is the frequency f or the time t, x_0 is the central frequency f_0 or the time t_0, dx is the bandwidth df or the transient time dt, A_x is the amplitude A_f or A_t.

The families of characteristics (Fig. 5) show that frequency and time responses are closest to Gaussian functions for the channels consisting of five PF (Fig. 5c). The lateral interactions of PF allow using the filters with lower selectivity. A further increase in number of PF does not give a better approximation. The damping (multiplier h values) should be at least double of that estimated by (7) and shown in Table 1.

Table 1

Natural frequencies (Nat. Freq.), damping (Damp.) and signal summation weights for channels consisting of one (PF-1), three (PF-3), five (PF-5), seven (PF-7), nine (PF-9) and eleven (PF-11) PF

No.	Nat. freq.	Damp.	PF-1	PF-3	PF-5	PF-7	PF-9	PF-11
1	1244.70	0.0213	0	0	0	0	0	− 1
2	1191.70	0.0215	0	0	0	0	1	10
3	1140.50	0.0217	0	0	0	− 1	−8	− 45
4	1091.00	0.0219	0	0	1	6	28	120
5	1043.20	0.0221	0	−1	−4	−15	−56	−210
6	996.97	0.0224	1	2	6	20	70	252
7	952.35	0.0226	0	−1	−4	−15	−56	−210
8	909.25	0.0229	0	0	1	6	28	120
9	857.64	0.0232	0	0	0	− 1	−8	− 45
10	827.47	0.0234	0	0	0	0	1	10
11	788.69	0.0237	0	0	0	0	0	− 1

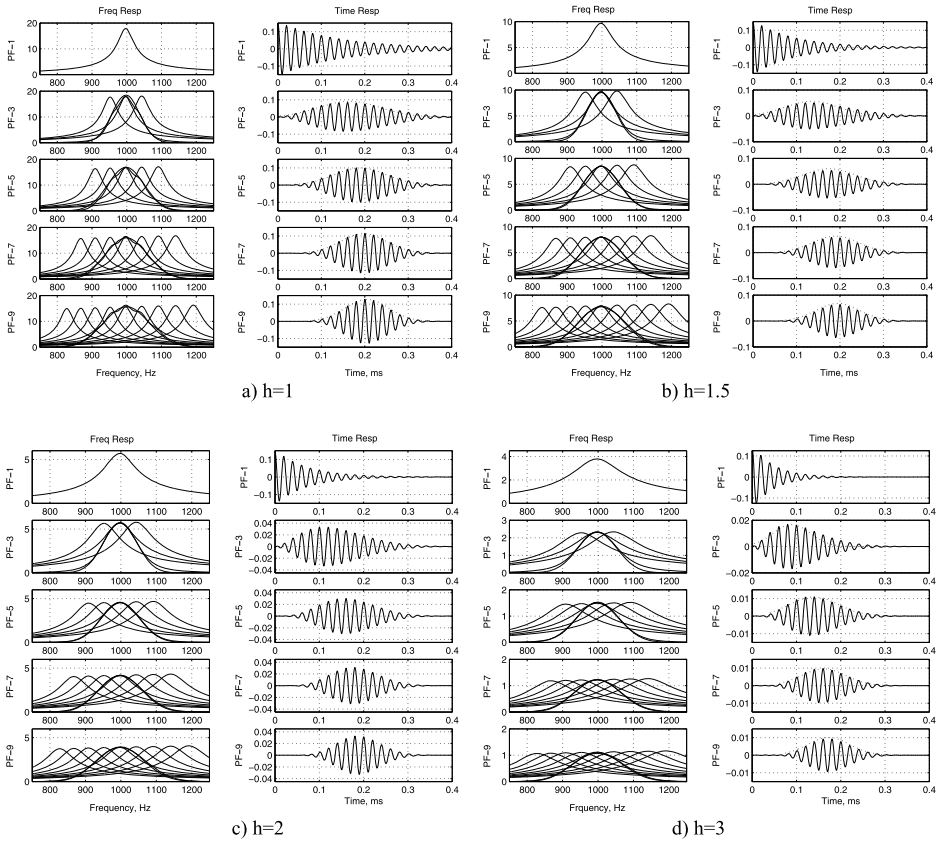

Fig. 5. Frequency and time response of filtering channels depending on the number of primary filters in a channel ($M = 1, 3, 5, 7, 9$) and on the damping multiplier ($h = 1; 1.5; 2; 3$).

4. Panoramic Gaussian Filter Bank

Encoding of the sound frequency in the cochlea is based on the place and time principle. The place principle means that each frequency evokes maximal displacement in a "characteristic place" of the BM (von Bekesy, 1960; Robles *et al.*, 2001). Therefore the position of the OHC on the BM and the natural frequency of the corresponding PF are interrelated. The place of origin of a nerve fiber determines its "characteristic frequency", i.e., the sound frequency to which it is most responsive. Consequently, the filtering system of the cochlea is three-dimensional (panoramic). Therefore impulses generated by a cochlear implant and conducted through electrodes implanted in the cochlea should excite the auditory fibers in the appropriate place. A deviation of central frequencies of the implant filter bank from appropriate biological places in the cochlea worsens significantly understanding of speech (Fu *et al.*, 1999). Therefore in clinical practice a correction of the channel frequencies may be necessary taking into account individual peculiarities of hearing in a patient, inaccuracy of placement due to a limited number of electrodes or

equal intervals between them. In our model (Fig. 4) the central frequencies of the filtering channels are distributed according to their biological place in the cochlea (Table 2).

In a given frequency range channels can be formed with common lateral PF or autonomously. The formation of channels with the common lateral PF (Fig. 4) allows sparing a number of them. For example, in a channel consisting of five filters the number of PF is $2N + 3$ instead of the number $5N$ used for autonomous realization, where N is the number of channels. Moreover, the structure of the filter bank channels is simplified by ignoring the delay of the excitation signal in the cochlea and the inertia of RM. The amplitude responses of a filter bank consisting of 20 Gaussian channels spanning the ranges of 250–2,100 Hz and 2,000–10,000 Hz are shown in Fig. 6. In order to assess changes in

Table 2

Natural frequencies (Nat Freq), damping factors (Damp) of the PF, summation weights in the channel and the location (Lk) of PF in the cochlea

No.	Nat Freq	Damp.	Channels of the filter bank (M = 5; N = 20)																			Lk
			1	2	3	4	5	6	7	8	9	10	11	12	13	14	15	16	17	18	19	20	
1	11215.0	0.0351	1																				4.36
2	10452.0	0.0354	−4																				4.86
3	9734.9	0.0357	6	1																			5.36
4	9061.0	0.0360	−4	−4																			5.87
5	8428.2	0.0364	1	6	1																		6.39
6	7834.3	0.0367		−4	−4																		6.91
7	7277.1	0.0371		1	6	1																	7.43
8	6754.8	0.0374			−4	−4																	7.96
9	6265.3	0.0378			1	6	1																8.49
10	5806.8	0.0382				−4	−4																9.02
11	5377.6	0.0386				1	6	1															9.56
12	4976.0	0.0390					−4	−4															10.11
13	4600.6	0.0394					1	6	1														10.66
14	4249.7	0.0399						−4	−4														11.21
15	3921.9	0.0404						1	6	1													11.77
16	3616.0	0.0409							−4	−4													12.33
17	3330.6	0.0414							1	6	1												12.90
18	3064.5	0.0419								−4	−4												13.47
19	2816.6	0.0425								1	6	1											14.05
20	2585.7	0.0431									−4	−4											14.63
21	2370.9	0.0437									1	6	1										15.22
22	2171.1	0.0444										−4	−4										15.82
23	1985.5	0.0451										1	6	1									16.42
24	1813.1	0.0458											−4	−4									17.02
25	1653.0	0.0466											1	6	1								17.63
26	1504.6	0.0475												−4	−4								18.25
27	1367.1	0.0484												1	6	1							18.87
28	1239.7	0.0494													−4	−4							19.50
29	1121.8	0.0505													1	6	1						20.13
30	1012.9	0.0517														−4	−4						20.77
31	912.1	0.0530														1	6	1					21.42
32	819.1	0.0545															−4	−4					22.07
33	733.3	0.0561															1	6	1				22.73
34	654.3	0.0580																−4	−4				23.40
35	581.5	0.0601																1	6	1			24.07
36	514.5	0.0624																	−4	−4			24.76
37	452.9	0.0652																	1	6	1		25.44
38	396.3	0.0684																		−4	−4		26.14
39	344.4	0.0722																		1	6	1	26.84
40	296.7	0.0768																			−4	−4	27.55
41	253.1	0.0824																			1	6	28.27
42	213.2	0.0895																				−4	29.00
43	176.7	0.0986																				1	29.73

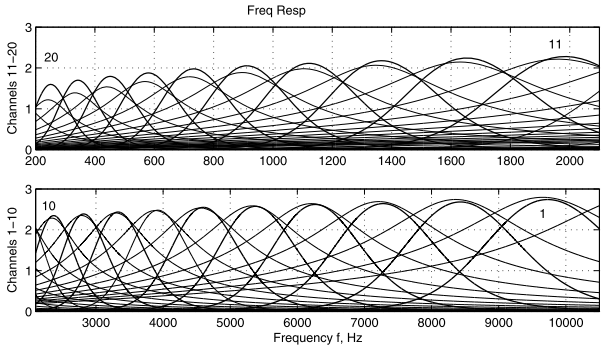

a) h=3.55

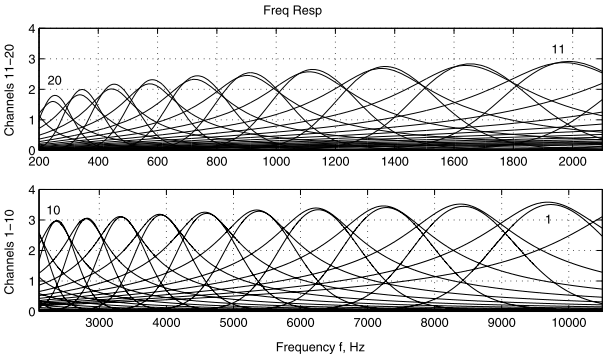

b) h=2.95

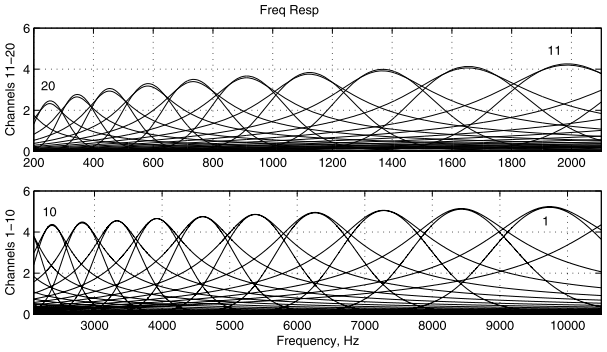

c) h=2.85

Fig. 6. Frequency responses of the Gaussian filter bank consisting of 20 channels (responses of higher selectivity) and of their central PF (responses of lower selectivity). Natural frequencies of the PF are given in Table 2. The values of damping for Gaussian channels are h times larger than those given for the PF in the table. The values h were found by computer modeling: the damping multiplier h was varied until the maxima of the frequency responses of both the channels and their central PF became approximately the same. (a) $h = 3.55$ for Gaussian channels with the signal delay in the cochlea and inertia of the RM. (b) $h = 2.95$ for channels without delay. (c) $h = 2.85$ for channels consisting only of the PF.

channel characteristics, we modeled three cases: (1) the effect of the delay, the influence of RM and the role of the filtering properties of the PF (Fig. 6a); (2) the influence of RM and the role of the filtering properties of the PF (Fig. 6b); (3) the role of the filtering properties of the PF only (Fig. 6c). The delay values τ_k of the filter bank are inversely proportional to the natural corner frequencies (12) and those of the local structures of RM and PF are equal (13). They are determined in the range 16–20,000 Hz with 56 PF. Only 43 PF are needed for 20 Gaussian channels in the range of 250–10,000 Hz. Their parameters are given in Table 2.

When designing the channels, the output signals of the PF are summed up with the weights suitable to form channels consisting of five PF. Their damping values are h times larger than those given in Table 2. When the channels consist of the PF only ($h = 2.85$), the maxima of their responses and those of the central PF coincide approximately throughout the whole range of frequencies (Fig. 6c). When designing the channels, the natural frequencies and initial damping of the PF correspond to the linear mode with the highest sensitivity and selectivity. If the PF used in our model are non-linear and their structure is the same as primary filtering circuits (PFC) in our previous work (Stasiunas *et al.*, 2009), then the properties of the present model in the nonlinear-adaptive mode can be deduced from the properties of the PFC. On the basis of these properties it can be expected that the sensitivity and selectivity of the channels will decrease at higher-level signals, and a band-pass will appear in the region of the double central frequency.

5. Discussion and Conclusions

In our previous works (Stasiunas *et al.*, 2003, 2005, 2008, 2009), we considered that the passive local structures of the cochlea together with the active OHC form the PF of the second order. The number of the PF corresponds to the number of the OHC. The output signals of the filtering channels consisting of the PF exert their action on the hairs of the IHC. The number of the channels corresponds to the number of the IHC. Following these assumptions, we proposed the structure of a serial-parallel multichannel filtering system consisting of the PF as a model of the signal filtering system of the cochlea. However, our view on the biological filtering system of the cochlea as well as the method of qualitative functional-computer modeling used by us (Stasiunas *et al.*, 2008, 2009), can be the object of discussion.

In the present work, we introduced the delay of the signal propagation in the cochlea and the influence of the RM (Fig. 4) in the filtering structure proposed by us previously. We estimated a possible distribution of the central frequencies of the biological filtering channels along the cochlea, a rational number of the PF comprising the Gaussian channels, and evaluated natural frequencies and damping factors of the PF comprising the channels of the Gaussian filter bank.

1. The distribution of the PF and their constituent OHC. We proposed a biologically-grounded recurrent algorithm for determining positions of the OHC on the BM (1)–(3). It is based on the assumptions that the OHC are hexagonally arranged

on the BM, and the BM widens toward the apex of the cochlea non-linearly but exponentially. Since the data about the character of widening of the BM are lacking we modeled the cases with a linear and exponential widening and considering distances between the neighboring OHC as constant, or increasing linearly or non-linearly. Using the recurrent algorithm and computer modeling we determined the number of the OHC contained in the middle row and distances between the neighboring OHC starting from the stapes (Fig. 2). The results of modeling show that the BM could contain the greatest number of the OHC with equal distances between them. However, we believe that exponential widening of the BM and non-linear change in distances between the OHC are more feasible biologically. By determining the locations of the OHC we determined the locations of the PF as well, since the OHC are the active elements of the PF.

2. The distribution of the natural frequencies and damping of the PF in the primary filter bank. We modified the dependence (4) of the CF on longitudinal position on the mammalian BM determined by Greenwood (Greenwood, 1990) for oscillations evoked by sine signals. Assuming that the CF correspond approximately to the natural frequencies of the PF, we determined the distribution of the natural frequencies of the PF (5) according the position of the OHC in the cochlea (Fig. 3). Assuming that the distance between the neighboring natural frequencies corresponds to the bandwidth of the PF, we determined the quality (6) and damping (7) of the PF. When the positions of the PF in the cochlea, their natural frequencies and damping are estimated, it is possible to design a primary panoramic filter bank. The frequency responses of a part of such a bank consisting of 56 PF and spanning the frequency range of 16–20,000 Hz are shown in Fig. 3. The frequency responses intersect at the level of 0.7. The quality of the constituent PF depends on the frequency range and the number of the PF in the bank.
3. Estimation of a rational number of the PF and their damping in a Gaussian channel. Gaussian filters are distinctive in their frequency selectivity and short transient process. We tried to form the channels with Gaussian time and frequency responses. We design the channels consisting of 1, 3, 5, 7 and 9 PF. We compared their frequency and time responses obtained by computer modeling with the graphs of Gaussian frequency and time functions (Fig. 5). By changing the damping, we determined that the responses are closest to the Gaussian function when the channel consists of five PF and their damping is at least double of that estimated by (7). It may be concluded that the channels of the filtering system of the cochlea can be of the tenth order and Gaussian type.
4. Formation of the secondary Gaussian panoramic filter bank. We designed a filter bank operating in the linear mode for the highest sensitivity and selectivity. The channels of the filter bank in the selected frequency range can be formed with the common lateral PF or autonomously. Smaller number of PF is needed to form filter banks with the common lateral PF of the channels. For example, when a Gaussian channel consists of five filters and number of channels is N, then only the number $2N + 3$ of the PF is needed instead of the number $5N$ used for autonomous realization. Moreover, such channels are more reliable since the neighboring channels

continue functioning (although with some deviations) if one channel is out of order. Hence, hearing in some frequency range can be impaired due to defective OHC in the cochlea (Janušauskas *et al.*, 2010). If the excitation signal delay in the cochlea and the inertia of RM are ignored the structure of channels becomes simplified. Modeling results obtained with a panoramic filter bank consisting of 20 channels show (Fig. 6) that responses of such channels (Fig. 6c) differ only a little from those which are more adequate biologically (Fig. 6a). It may be concluded that the structure of the panoramic filter banks with the common PF of the neighboring channels of the tenth order and Gaussian type is closest to biological principles.

5. Application of the results. Our model can be useful in designing panoramic filter banks for cochlear implants (Gao *et al.*, 2003; Wilson *et al.*, 2005; Zeng *et al.*, 2008). The strategy of signal processing used in cochlear implants at present time is oriented more to the properties of the speech signals (Zeng *et al*., 2008) than to the biological principles of signal processing in the cochlea of the inner ear. It may be expected that the design of cochlear implants could be improved by harmonizing the biological principles of signal processing with the properties of the speech signal. From this point of view the proposed biologically based and economical design of a panoramic Gaussian filter-bank may be useful for the new speech coding strategies.

Acknowledgements. We gratefully acknowledge the support from the Research Council of Lithuania; grant number MIP-46/2010.

References

Allen, J.B. (1979). Cochlear models – 1978. *Scandinavian Audiology Supplement*, 9, 1–16.

Ashmore, J.F. (1987). A fast motile response in guinea-pig outer hair cells: The cellular basis of the cochlear amplifier. *Journal of Physiology*, 388, 326–347.

Ashmore, J.F. (2008). Cochlear outer hair cell motility. *Physiological Reviews*, 88(1), 173–210.

von Bekesy, G. (1960). *Experiments in Hearing*. McGraw-Hill, New York.

Boron, W.F., Boulpaep, E.L. (2003).*Medical Physiology: A Cellular and Molecular Approach*. Saunders, Philadelphia.

Brownell, W.E., Bader, C.R., Bertrand, D., de Ribaupierre, Y. (1985). Evoked mechanical responses of isolated cochlear outer hair cells. *Science*, 227, 194–196.

Chan, D.K., Hudspeth, A.J. (2005a). Ca2+ current-driven nonlinear amplification by the mammalian cochlea in vitro. *Nature Neuroscience*, 8(2), 149–155.

Chan, D.K., Hudspeth, A.J. (2005b). Mechanical responses of the organ of corti to acoustic and electrical stimulation in vitro. *Biophysical Journal*, 89(6), 4382–4395.

Clark, G.M. (2006). The multiple-channel cochlear implant: the interface between sound and the central nervous system for hearing, speech, and language in deaf people – a personal perspective. *Philosophical Transactions of Royal Society B.*, 361, 791–810.

Crawford, A.C., Fettiplace, R. (1985). The mechanical properties of ciliary bundles of turtle cochlear hair cells. *Journal of Physiology*, 364, 359–379.

Dallos, P. (2008). Cochlear amplification, outer hair cells and prestin. *Current Opinion in Neurobiology*, 18(4), 370–378.

Dallos, P., Evans, B.N. (1995). High frequency motility of outer hair cells and the cochlear amplifier. *Science*, 267, 2006–2009.

Dallos, P., Zheng, J., and Cheatham M.A. (2006). Prestin and the cochlear amplifier. *Journal of Physiology*, 576.1, 37–42.

Dallos, P., Wu, X., Cheatham, M.A., Gao, J., Zheng, J., Anderson, C.T., Jia, S., Wang, X., Cheng, W.H., Sengupta, S., He, D.Z., Zuo, J. (2008). Prestin-based outer hair cell motility is necessary for mammalian cochlear amplification. *Neuron*, 58(3), 333–339.

Davis, H. (1983). An active process in cochlear mechanics. *Hearing Research*, 9(1), 79–90.

Evans, M.G., Kros, C.J. (2006). The cochlea – new insights into the conversion of sound into electrical signals. *Journal of Physiology*, 576(Pt 1), 3–5.

Evans, B.N., Dallos, P. (1993). Stereocilia displacement induced somatic motility of cochlear outer hair cells. *Proceedings of the National Academy of Sciences of USA*, 90(18), 8347–8351.

Frank, G., Hemmert, W., Gummer, A.W. (1999). Limiting dynamics of high-frequency electromechanical transduction of outer hair cells. *Proceedings of the National Academy of Sciences of USA*, 96, 4420–4425.

Fridberger, A., de Monvel, J.B., Zheng, J., Hu, N., Zou, Y., Ren, T., and Nuttall, A. (2004). Organ of Corti potentials and the motion of the basilar membrane. *Journal of Neuroscience*, 24(45), 10057–10063.

Fu, Q.J., Shannon, R.V. (1999). Effects of electrode configuration and frequency allocation on vowel recognition with the Nucleus-22 cochlear implant. *Ear and Hearing*, 20(4), 332–344.

Gao, R., Basseas, S., Bargiotas, D.T., and Tsoukalas, L.H. (2003). Next-generation hearing prosthetics, *IEEE Robotics & Automation Magazine*, March, 21–25.

Gold, T. (1948). Hearing II. The physical basis for the action of the cochlear. *Proceedings of Royal Society of London B., Biology Sciences*, 135, 492–498.

Greenwood, D.D. (1990). A cochlear frequency-position function for several species – 29 years later. *Journal of Acoustical Society of America*, 87, 2592–2605.

Greenwood, D.D. (1996). Comparing octaves, frequency ranges, and cochlear-map curvature across species, *Hearing Research*, 94, 157–162.

Hudspeth, A.J., Corey, D.P. (1997). Sensitivity, polarity, and conductance change in the response of vertebrate hair cells to controlled mechanical stimuli, *Proceedings of the National Academy of Sciences of USA*, 74(6), 2407–2411.

Janušauskas, A., Marozas, V., Lukoševičius, A., Sornmo, L. (2010). Detection hearing loss in audiological frequencies from transient evoked otoacoustic emissions. *Informatica*, 21(2), 191–204.

Jia, S., He, D.Z. (2005). Motility-associated hair-bundle motion in mammalian outer hair cells. *Nature Neuroscience*, 8(8), 1028–1034.

Kemp, D.T. (1978). Stimulated acoustic emissions from within the human auditory system. *Journal of Acoustic Society of America*, 64, 1386–1391.

Kennedy, H.A., Crawford, A.C., Fettiplace, R. (2005). Force generation by mammalian hair bundles supports a role in cochlear amplification. *Nature*, 433(2), 880–883.

Kennedy, H.J., Evans, M.G., Crawford, A.C., Fettiplace, R. (2006). Depolarization of cochlear outer hair cells evokes active hair bundle motion by two mechanisms. *Journal of Neuroscience*, 26(10), 2757–2766.

Lu, T.K., Zhak, S., Dallos, P., Sarpeshkar, R. (2006). Fast cochlear amplification with slow outer hair cells. *Hearing Research*, 214(1–2), 45–67.

Manley, G.A. (2001). Evidence for an active process and a cochlear amplifier in nonmammals. *Journal of Neurophysiology*, 86(2), 541–549.

Neely, S.T., Kim, D.O. (1983). An active cochlear model showing sharp tunning and high sensitivity. *Hearing Research*, 9, 123–130.

Nobili, R., Mammano, F., Ashmore, J. (1998). How well do we understand the cochlea? *Trends of Neurosciences*. 21(4), 159–67.

Preyer, S., Renz, S., Hemmert, W., Zenner, H.-P., Gummer, A.W. (1996). Receptor potential of outer hair cells isolated from base to apex of the adult guinea-pig cochlea: implications for cochlear tuning mechanisms. *Auditory Neuroscience*, 2, 145–157.

Rhode, W.S. (1971). Observations of the vibration of the basilar membrane in squirrel monkeys using the Mössbauer technique. *Journal of Acoustical Society of America*, 49, 1218–1231.

Ricci, A. (2003). Active hair bundle movements and cochlear amplifier. *Journal of Americal Academy of Audiology*, 14(8), 325–338.

Robles, L., Ruggero, M.A. (2001). Mechanics of the mammalian cochlea. *Physiology Review*, 81(3), 1305–1352.

Russell, I.J., Sellick, P.M. (1983). Low-frequency characteristics of intracellularly recorded receptor potentials in guinea-pig cochlear hair cells. *Journal of Physiology*, 338, 179–206.

Santos-Sacchi, J. (1992). On the frequency limit and phase of outer hair cell motility: effects of the membrane filter. *Journal of Neuroscience*, 12(5), 1906–1916.

Scherer, M.P., Gummer, A.W. (2004). Vibration pattern of the organ of Corti up to 50 kHz: evidence for resonant electromechanical force. *Proceedings of the National Academy of Sciences of USA*, 21(101), 17652–17657.

Spector, A.A., Brownell, W.E., Popel, A.S. (1999). Mechanical and electromotile characteristics of auditory outer hair cells. *Medical and Biological Engineering and Computing*, 37(2), 247–251.

Standring, S. (Ed.) (2005). *Gray's Anatomy: The Anatomical Basis of Clinical Practice*, 39th edn. Elsevier/Churchill/Livingstone, Edinburgh/New York.

Stasiunas, A., Verikas, A., Kemesis, P., Bacauskiene, M., Miliauskas, R., Stasiuniene, N., Malmqvist, K. (2003). A non-linear circuit for simulating OHC of the cochlea. *Med Eng. Phys.* 25(7), 591–601.

Stasiunas, A., Verikas, A., Bacauskiene, M., Miliauskas, R., Stasiuniene, N., Malmqvist, K. (2005). Compression, adaptation and efferent control in a revised outer hair cell functional model. *Medical Engineering & Physics*, 27(9), 780–789.

Stasiunas, A., Verikas, A., Miliauskas, R., Stasiuniene, N., Bacauskiene, M. (2008). Physiologically inspired signal preprocessing for auditory prostheses: insights from the electro-motility of the OHC. *Medical Engineering & Physics*, 30(2), 171–181.

Stasiunas, A., Verikas, A., Miliauskas, R., Stasiuniene, N. (2009). An adaptive model simulating the somatic motility and the active hair bundle motion of the OHC. *Computers in Biology and Medicine*, 39(9), 800–809.

Sugawara, M., Wada, H. (2001). Analysis of elastic properties of outer hair cell wall using shell theory (1). *Hearing Research*, 160(1–2), 63–72.

Wilson, B.S., Schatzer, R., Lopez-Poveda, E.A., Sun, X., Lawson, D.T., Wolford, R.D. (2005). Two new directions in speech processor design for cochlear implants. *Ear and Hearing*, 26(4 Suppl), 73S–81S.

Zeng, F.-G., Rebscher, S., Harrison, W.V., Sun, X., and Feng, H. (2008). Cochlear implants: system design, integration and evalution. *IEEE Reviews in Biomedical Engineering*, 1, 115–142.

Zhao, H.-B., Santos-Sacchi, J. (1999). Auditory collusion and coupled couple of outer hair cells. *Nature*, 399(5), 359–362.

Zheng, J., Shen, W., He, D.Z., Long, K.B., Madison, L.D., Dallos, P. (2000). Prestin is the motor protein of cochlear outer hair cells. *Nature*, 405(6783), 149–155.

Zwicker, E. (1979). A model describing nonlinearities in hearing by active processes with saturation at 40 dB. *Biological Cybernetics*, 35(4), 243–250.

A. Stasiūnas received his PhD degree in signal processing in 1971 from Kaunas University of Technology, Lithuania. He became associate professor at the same university (Department of Control Systems) in 1978. His research interests include signal transmission and processing, process control, speech and hearing system analysis.

A. Verikas is currently holding a professor position at both Halmstad University Sweden and Kaunas University of Technology, Lithuania. His research interests include image processing, pattern recognition, neural networks, fuzzy logic, and visual media technology. He is a member of the International Pattern Recognition Society, European Neural Network Society, and a member of the IEEE.

R. Miliauskas received his PhD degree in neurophysiology in 1970 from Kaunas University of Medicine, Lithuania. He became associate professor at the same university in 1993. The main field of his scientific interests is the electrical activity of the brain and nerve cells.

M. Bačauskienė is a senior researcher in the Department of Electrical and Control Equipment at Kaunas University of Technology, Lithuania. Her research interests include artificial neural networks, image processing, pattern recognition, and fuzzy logic. She participated in various research projects and published numerous papers in these areas.

Nuoseklus-lygiagretus panoraminis filtrų bankas, kaip sudėtingų garsų dažnių dekompozicijos žmogaus vidinėje ausyje modelis

Antanas STASIŪNAS, Antanas VERIKAS, Rimvydas MILIAUSKAS, Marija BAČAUSKIENĖ

Sudarydami modelį, mes laikėme, kad vidinės ausies sraigės išorinės plaukuotosios ląstelės kartu su vietinėmis pamatinės plokštelės struktūromis, tinkline membrana ir dengiamąja membrana sudaro antros eilės pirminius filtrus (PF). Mes sudarėme nuoseklią-lygiagrečią signalų filtracijos sistemą su bendrais gretimų kanalų PF, įvertinant žadinimo signalo sklidimo vėlinimą sraigėje ir Reisnerio membranos įtaką. Nustatėme kanalų centrinių dažnių išsidėstymą išilgai sraigės, gausinį kanalą sudarančių PF optimalų skaičių, jų savuosius dažnius, slopinimo faktorius, PF išėjimo signalų sumavimo svorius. Pagal mūsų pasiūlytą metodiką, kaipo pavyzdį, sudarėme filtrų banką iš 20 gausinio tipo kanalų, susidedančių iš penkių PF ir nustatėme jų dažnines charakteristikas. Pasiūlytoji signalų filtracijos sistema gali būti naudinga, kuriant klausos implantams biologiškai pagrįstas kalbos kodavimo strategijas.